VISUALIZATION AND ANALYSIS OF VISCOUS FLUID FLOW IN SPHERICAL COUETTE SYSTEM

Kazuki Yoshikawa[1*], Kazuyuki Nakagawa[2], Isshin Arai[2], Kazuki Sakakibara[2] and Tomoaki Itano[2]

(Received September 1, 2023; accepted January 16, 2024)

Abstract:

The flow of a Newtonian fluid confined between concentric double spheres, with a stationary outer sphere and an inner sphere rotating at a constant angular velocity, is referred to as spherical Couette flow (SCF). The equilibrium state of SCF is determined by the radius ratio of the inner to outer spheres, η, and the Reynolds number, Re. For $\eta \leq 0.75$, when Re exceeds the critical Reynolds number, Re_c, a flow characterized by high shear regions extending from the poles to the equatorial zone appears at the first transition. This transitional flow is known as the spiral state. In this study, the spiral state is visualized and analyzed at a radius ratio of η=0.5. By analyzing the brightness of the captured images, a period unique to the spiral state was confirmed, and the frequency distribution reveals the existence of two patterns with different wavenumbers.

1 Introduction

The cores of many astronomical bodies are hypothesized to be fluid-filled systems confined within concentric double spherical boundaries. Typically, these boundaries, corresponding to the inner and outer spheres, rotate at different angular velocities[1]. An illustrative example is the Earth, where a liquid outer core is confined between a solid inner core and a mantle. The fluid dynamics within these astronomical bodies are affected by various factors, including the Coriolis force, thermal instability, gravity, and the Lorentz force via electromagnetic fields. In this study, we employ a simple model involving a Newtonian fluid flow between concentric double spherical shells. In this model, the inner sphere rotates at a constant angular velocity while the outer sphere remains stationary. This fluid flow is termed spherical Couette flow (SCF), and the resultant flow pattern is known to be determined by the radius ratio, $\eta=R_{in}/R_{out}$, and the Reynolds number, $Re=R_{in}^2\,\Omega_{in}/\nu$, where R_{in}, and R_{out} are the radii of the inner and outer spheres, respectively, Ω_{in} is the angular velocity of the inner sphere, and ν is the kinematic viscosity of the working fluid.

Egbers and Rath[2] investigated SCF transitions, both numerically and experimentally, at various radius ratios. For a relatively wide gap between the inner and outer spheres with a radius ratio of $\eta \leq 0.75$, their experiments revealed the transition from axisymmetric flow to

1 Graduate School of Science and Engineering, Kansai University, Suita, Osaka 564-8680, Japan
2 Department of Engineering Science, Kansai University, Suita, Osaka 564-8680, Japan
* Correspondence to: Kazuki Yoshikawa, Graduate School of Science and Engineering, Kansai University, Suita, Osaka 564-8680, Japan. E-mail: k320126@kansai-u.ac.jp

turbulent flow via spiral waves, commonly referred to as the spiral state. In their experiments at η=0.5, this transition from axisymmetric flow to the spiral state was observed around Re=490[3]. To analyze the flow transition, they used a laser doppler velocimeter (LDV) to measure the one-dimensional velocity field of the flow.

In the present study, we visualized the flow field in SCF at η=0.5 and analyzed the time variation of the flow pattern in the spiral state. This was achieved using aluminum flakes and a laser light sheet projected into the flow. In the spiral state, the luminance reflected by the aluminum flakes is expected to vary periodically over time, with its frequency uniquely determined by the rotation angular velocity of the inner sphere. Previous studies by our group confirmed the robust presence of the spiral state in the range of Re<800 using this approach. Additionally, Yoshikawa et al.[7] demonstrated that the visualized flow in the spiral state can be reproduced numerically. However, it remains uncertain whether the same spiral state can be observed at larger Reynolds numbers. Therefore, the objective of this study is to confirm whether the spiral state can be realized in the range of 800<Re. Section 2 provides a detailed explanation of our experimental setup, followed by the presentation of results in the successive section. In Section 4, we engage in a discussion comparing the present experimental results with previous numerical solutions.

2 Experimental setup

We fabricated an aluminum inner sphere anodized black with radius R_{in}=42.5 [mm] and an acrylic outer sphere with radius R_{out}=85.0 [mm] to satisfy the radius ratio of η=0.5. The space between the spheres was filled with a typical 20 to 30 wt% aqueous glycerol solution, with a density of approximately ρ_{gw}=1.05 to 1.09 [g/cm^3]. Aluminum flakes (Daiwa Metal Powder Co., No.1112, average particle diameter of 23 μm, ρ_{Al}=2.70[g/cm^3]) were mixed as tracer particles for visualization. On the upper pole side of the outer sphere, a small hole with a 6.5 mm diameter was created, allowing the inner sphere to be suspended on a shaft with a 6.0 mm diameter. The shaft is connected to a brushless DC motor (Oriental Motor, GFS2G5, BXM230-GFS, BXSD30-A), providing control over the angular velocity Ω_{in} of the inner sphere.

To visualize the flow, a laser sheet (laser source: Integrated Optics, 0520 L-11A, CW 520 nm / 200 mW) was projected onto a plane vertical to the axis of rotation of the sphere. The laser sheet's plane was positioned at a height tangent to the top of the inner sphere (z=42.5 [mm]), and the flow pattern was captured by a camera (Sony, DSC-RX0M2) from the polar side (Fig. 1). Due to the thin plate-like shape of aluminum flakes, there is a possibility of laser light reflection in the direction of the camera. As the laser light passed from the air to the acrylic container and the fluid, it underwent slightly refraction in the direction of the z-axis. However, this refraction is considered negligible.

This experiment was carried out according to the following procedure. First, the temperature of the fluid was measured with the inner sphere at rest. Subsequently, the inner sphere was rotated at a constant angular velocity, maintained for more than 40 min. Upon confirming that the fluid flow had sufficiently developed into an equilibrium state, the flow was recorded using a camera for a duration of 6 min. The camera had a resolution of 1920×1080 pixels (approximately 0.1 mm/pixel), and the frame rate was set at 24 fps. After

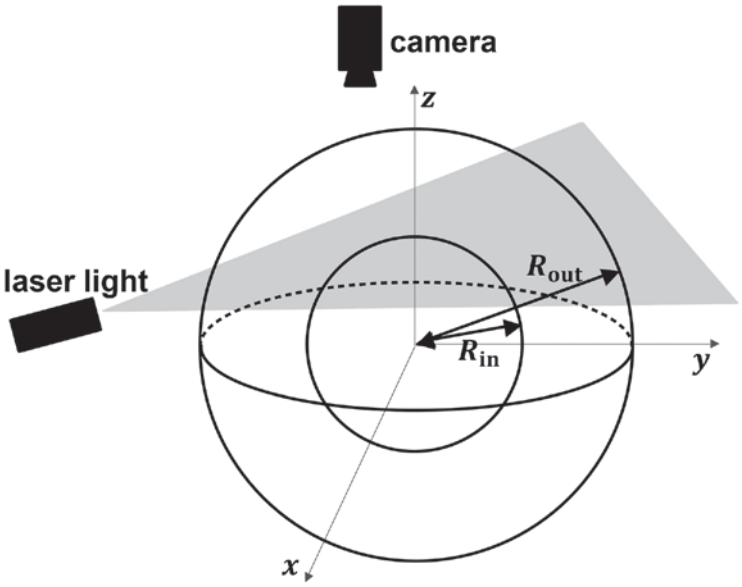

Fig. 1. This illustration depicts the projection of a laser sheet to visualize spherical Couette flow. The z-axis corresponds to the axis of rotation of the inner sphere, and the laser sheet is projected onto a plane vertical to the axis. The inner sphere has a radius of R_{in}=42.5 [mm], the outer sphere has a radius of R_{out}=85.0 [mm], and laser sheet's plane is z=42.5 [mm]. Aluminum flakes were mixed with the working fluid.

recording was complete, the rotation of the inner sphere was halted and it remained at rest for 5 min. The temperature of the fluid was then measured once more. The temperature of the fluid during the experiment was considered as the average of the initial and final measured temperatures, with the temperature difference falling within ±0.5 deg. The kinematic viscosity, ν, of the aqueous glycerol solution and the Reynolds number, $Re=R_{in}^{2}\,\Omega_{in}/\nu$, were calculated based on the measured temperatures[4]. Experiments were conducted within the Reynolds number range of $Re\geqq480$, and the flow state transition was also investigated.

3 Experimental Results

First, the experiment was conducted at low Reynolds numbers. There was no significant change in the flow pattern up to Re=500, and the brightness of the reflected light from the aluminum flakes did not change over time. Figure 2 consists of snapshots of the flow at Re=598. The snapshots were taken every 6 s, revealing a repeating light and dark pattern with a period of approximately 18 s. In these snapshots, the center of rotation is positioned at the bottom of the figures, and the outer sphere is observed on the upper side, with the flow streaming counterclockwise. In Fig. 2(a), a bright streaky area extends from the shaft at the center of rotation, accompanied by a circular dark area slightly closer to the outer sphere. This dark area moves in the streamwise direction over time. After its passage, the entire area remains bright for a while (Fig. 2(b), (c)). Subsequently, a new dark shadow emerges, featuring a circular dark area similar to the one observed in Fig. 2(a) (Fig. 2(d)). This periodic change in the light and dark pattern is evident within the Reynolds number range up to Re=801. With further increases in the Reynolds number, the periodic change becomes

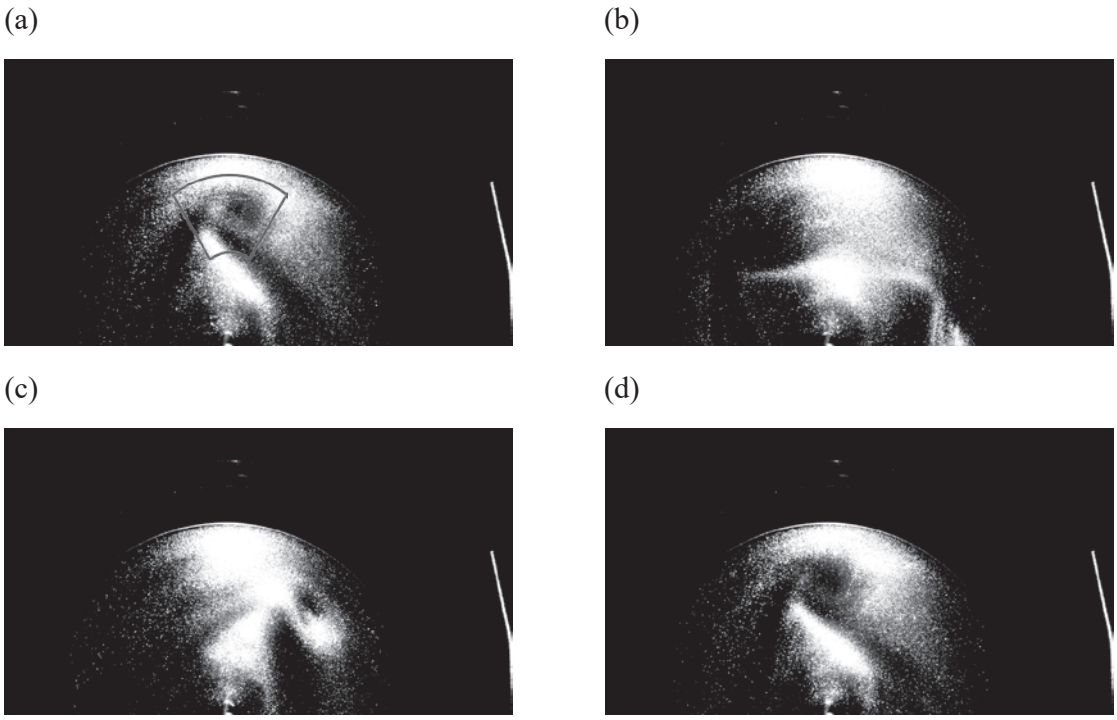

Fig. 2. Aluminum flakes mixed in the working fluid reflect the laser light. Recording was carried out at 24 fps for 6 min, with snapshots (a) to (d) taken every 6 s. In these snapshots, the shaft at the center of rotation is visible at the bottom, and the outer sphere is at the center. The luminance of the area enclosed by the solid line in (a) was analyzed.

slightly irregular, and the light and dark pattern gradually becomes more complex. To assess the period that was observed in the spiral state, the luminance of recorded snapshots was analyzed. The analysis focused on the luminance of the area shaped like a piece of baumkuchen with a 60° center angle and 150 pixels difference between outer and inner diameters, where the time variation of luminance was clearly visible. Figure 3(a) illustrates the luminance changes with time at Re=598, and the spectrum of the time variation of luminance, analyzed by Fourier transform, is shown in Fig. 3(b). The spectrum was confirmed a local peak at f_p=0.0586 [/s]. The light and dark pattern was observed with a period of approximately 17 s. These periodic changes were evident up to Re=1219.

Upon careful observation of the movement of the aluminum flakes compared with the light and dark patterns, it was noted that an aluminum flake is neither constantly shiny nor constantly dark. The aluminum flakes in the fluid reflect the laser light to the camera only when they are at a specific orientation due to the shear field of the flow. When the Reynolds number was small and the flow was axisymmetric, the particles generally appeared shiny and no dark areas were observed. This suggests that, in regions with strong shear in the spiral state, the aluminum flakes assume a particular orientation. In regions with weak shear, the particles take isotropic orientations, some of which reflect light in the direction of the camera. In the high shear region, most particles have a specific orientation and do not reflect light to the camera, resulting in the visibility of the light and dark pattern.

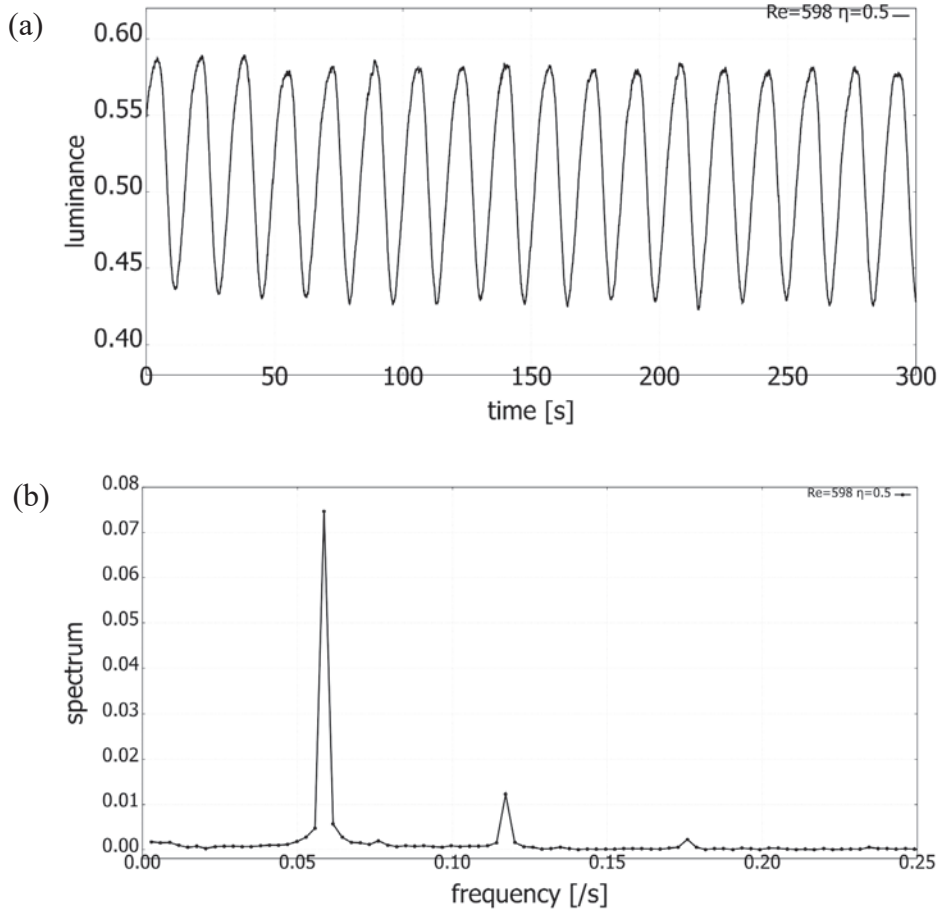

Fig. 3. (a) This figure represents the time series data of the luminance of the light reflected by aluminum flakes at Re=598. The luminance in the baumkuchen-shaped area was evaluated. (b) The spectrum of time variation of the luminance was analyzed by Fourier transform. A local peak at f_p=0.0586 is confirmed.

4 Discussion

In the SCF, a spiral state can be observed for a radius ratio $\eta \leq 0.75$ within a specific range of Reynolds numbers. The spiral state is characterized by high shear regions extending from both poles toward the equatorial plane. These regions allocate in an antisymmetric way in each hemisphere and periodically around the axis of rotation. The number, m, of high-shear regions in the flow depends on the gap width between the spheres; for η=0.5, spiral states with m=2, 3, and 4 have been observed. In this experiment visualizing the SCF, the mode of the confirmed spiral state is investigated based on the time series data of the luminance.

As illustrated in Fig. 2, at Re=598, the light and dark pattern appears periodic, and Fig. 3(a) shows that the luminance varies over time. The frequency, f, of the time variation was evaluated from the luminance's time series data, and the distribution of the dimensionless parameter, $2\pi f/\Omega_{in}$, was obtained. Figure 4 displays the distribution of the frequency, f, of the time variation at each Reynolds number. The present experimental results are denoted by triangles, and the solid or dashed lines represent values obtained from numerical calculations

[5][6]. In the numerical calculations, the flow velocity is expanded into a basic flow component based on the Stokes flow and a perturbation component. Since the perturbation component of the flow velocity is considered to affect the formation of the shear region, a dimensionless parameter is obtained from the angular velocity, ω, of the perturbation. The frequency of the spiral state observed at Re=520 ~ 600 and 801 is approximately equal to the numerically calculated value of m=3, while at Re=733 and 978 ~ 1219, the frequency of the spiral state is approximately equal to the value of m=2. This indicates that the number, m, of high shear regions in the spiral state tends to decrease as the Reynolds number increases. In this experiment, we could not confirm the dimensionless frequency corresponding to the m=4 spiral state.

An aluminum flake is a thin and flat plate, and the orientation of its face is determined by the shear field of the fluid. When shearing by the flow is strong, the orientations of the plates become aligned in a specific direction. In the spiral state in the SCF, there is a region of strong shear. Therefore, the light and dark pattern observed in this experiment is considered to be generated under the shear. Yoshikawa et al.[7] investigated the motion of an infinitesimal plane element suspended in a spherical Couette flow and numerically simulated the reflection of a projected laser sheet by the elements. It was found that both the circular dark areas and streaky bright areas observed in the experiment are realized in the simulation. The numerical

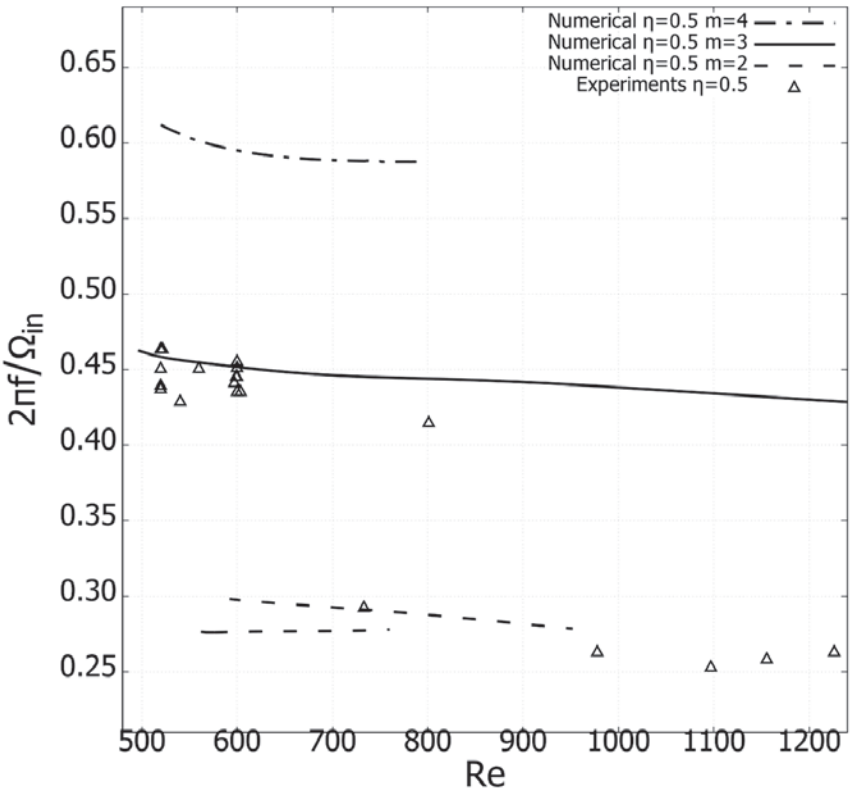

Fig. 4. The frequency distribution in the spiral state is plotted, with the Reynolds number on the x-axis and the dimensionless parameter, $2\pi f/\Omega_{in}$, where f is the frequency of the light and dark pattern and Ω_{in} is the angular velocity of the inner sphere on the y-axis.

reproduction of the visualized flow in the spiral state was simulated in the range of low Reynolds number. Therefore, periodic changes of the dark and light pattern in the experiment are expected to be confirmed by the same simulation in the range of higher Reynolds numbers.

5 Summary

In the present study, visualization experiments of spherical Couette flow were conducted. We investigated the range of Reynolds numbers over which the spiral state appears when the radius ratio of the inner and outer spheres is η=0.5. In this experiment, the behavior of the frequency characteristic of the spiral state was confirmed for Re=520 ~ 1200. The analysis of the frequency showed the existense of two patterns in its distribution. Comparing the frequency distributions with those obtained from numerical calculations, it was found that the spiral state is characterized by a wavenumber of m=2, 3. The results of the numerical calculation comparing the frequencies were examined by Goto et al.[6], for which we express our gratitude.

Acknowledgment

The authors would like to thank Mr. Kazuki Ota, Ms. Saki Tsumura, and Mr. Fumitoshi Goto for the pilot survey of the present study. This work was supported in part by the Grant-in- Aid for Scientific Research(C), JSPS KAKENHI, Grant No. 20K04294. This study also benefited from the interaction within RISE-2018 No. 824022 ATM2BT of the European Union Horizon 2020-MSCA program, which includes Kansai University.

References

[1] C. M. R. Fowler. The Solid Earth. Cambridge University Press, 2004.

[2] C. Egbers and H. J. Rath. The existence of Taylor vortices and wide-gap instabilities in spherical Couette flow. Acta Mechanica, 111:125–140, 1995.

[3] P. Wulf, C. Egbers, and H. J. Rath. Routes to chaos in wide-gap spherical Couette flow. Phys. Fluids, 11:1359–1372, 1999.

[4] N. Cheng. Formula for the viscosity of a glycerol-water mixture. Industrial Engineering Chemistry Research, 47:3285–3288, 2008.

[5] T. Itano and S. C. Generalis. Hairpin vortex solution in planar Couette flow: A tapestry of knotted vortices. Phys. Rev. Lett., 102:114501, 2009.

[6] F. Goto, T. Itano, M. Sugihara-Seki, and T. Adachi. Bifurcation aspect of polygonal coherence over transitional Reynolds numbers in wide-gap spherical Couette flow. Phys. Rev. Fluids, 6:113903, 2021.

[7] K. Yoshikawa, T. Itano and M. Sugihara-Seki. Numerical reproduction of the spiral wave visualized experimentally in a wide-gap spherical Couette flow. Phys. Fluids 35, 034110, 2023